Bethe's Wave-Function Revisited

Jacob Szeftel * and Jean-Claude Lévy

Posted Date: 2 April 2024

doi: 10.20944/preprints202404.0124.v1

Keywords: Lattice fermion models; Fermions in reduced dimensions

 doi:10.20944/preprints202404.0124.v1

Article

Bethe's Wave-Function Revisited

Jacob Szeftel and Jean-Claude Lévy

MPQ, UMR 7162, Université Paris Cité, 10 rue Alice Domont et Léonie Duquet, 75013 Paris
* Correspondence: szeftel.jacob@bbox.fr

Abstract: The *scattering* eigenstates of *any* Hamiltonian of electrons, coupled through a two-body force and moving on a one-dimensional lattice, are shown to be Bethe's wave-functions. The energy of the groundstate is compared with values, obtained previously for the Hubbard Hamiltonian by means of Bethe's wave-function and within the framework of the correlated Fermi gas. The same analysis is applied to electrons, interacting on neighbouring sites. The significance of those various groundstates is assessed with help of thermodynamics.

Keywords: lattice fermion models; fermions in reduced dimensions

---

1. Introduction

Bethe's wave-function was initially devised to diagonalise the Heisenberg[1,2] Hamiltonian for an infinite, one-dimensional ($d = 1$) lattice and was later extended[3,4] to the $d = 1$ Hubbard Hamiltonian. However, since those analyses resort heavily to technical peculiarities, associated with the concerned Hamiltonians, Bethe's wave-function could not be applied to any $d > 1$ model[5], nor to other $d = 1$ Hamiltonians. Therefore this article is aimed at showing that Bethe's wave-function gives access to the eigenspectrum of *every* realistic $d = 1$ Hamiltonian. Then the groundstate energy will be compared with data[6], obtained previously for the Hubbard Hamiltonian[3,4]. An additional comparison will be carried out with the data, resulting from the *correlated Fermi gas* model, introduced recently[7] to account for the properties of interacting electrons in normal metals. This method will be further applied to electrons interacting on neighbouring sites[8], which was believed so far to lie out of the scope of Bethe's wave-function[1–4].

Here is the outline : the proof of Bethe's wave-function being a many-electron eigenstate is laid out in section I and the general expression of the corresponding eigenvalue is worked out; the two-body scattering is studied in section II for two different $d = 1$ Hamiltonians, whereas section III will be concerned with the prominent role of a boundary condition; the groundstate energy, associated with each of the two mentioned models, is reckoned and compared with data, obtained by other methods, in sections IV and V; the various many-electron states, discussed here, are analysed comparatively in section VI; at last, the main results are summarised in the conclusion.

2. 1-Diagonalisation

Let us consider $n >> 1$ of electrons moving on a $d = 1$ lattice, comprising an *even* number $N >> 1$ of atomic sites, labelled by the index $i = 1, ..N$. The lattice parameter is taken equal to unity and each site can accommodate at most two electrons of opposite spin σ, which implies $n \leq 2N$. The Hamiltonian H, governing the electron motion, then reads

$$H = h_e + h_{e-e} \quad ,$$

wherein h_e, h_{e-e} describe the one-electron hopping between first neighbours and the two-electron interaction, respectively. Hence h_e reads[9]

$$h_e = -t \sum_{i,j,\sigma} \left(c^+_{i,\sigma} c_{j,\sigma} + c^+_{j,\sigma} c_{i,\sigma} \right) \quad ,$$

 doi:10.20944/preprints202404.0124.v1

wherein the sum is carried out over $\sigma = \pm 1$, $i = 1, ..N-1$ with $j = i+1$ and $c^+_{i,\sigma}, c_{i,\sigma}$ are one-electron creation and annihilation operators on the Wannier[9] state $|i,\sigma\rangle$

$$|i,\sigma\rangle = c^+_{i,\sigma}|0\rangle \quad , \quad |0\rangle = c_{i,\sigma}|i,\sigma\rangle \quad ,$$

with $|0\rangle$ referring to the no electron state. Then t designates the hopping integral

$$t = \left|\langle 0|c_{j,\sigma} V_{e-n} c^+_{i,\sigma}|0\rangle\right| \quad ,$$

with V_{e-n} standing for the electron-nucleus Coulomb potential. The resulting one-electron energy dispersion $\epsilon(k \in [-\pi, \pi])$ reads[9]

$$\epsilon(k) = -2t\cos k \quad . \tag{1}$$

h_{e-e} will be referred to as h_0, h_1 for two electrons sitting on the same site, which characterises the Hubbard model, or on first neighbours. They read[8]

$$\begin{aligned}
h_0 &= U_0 \textstyle\sum_{i=1}^{N} c^+_{i,\sigma} c^+_{i,-\sigma} c_{i,-\sigma} c_{i,\sigma} \\
U_0 &= \langle 0|c_{i,-\sigma} c_{i,\sigma} V_{e-e} c^+_{i,\sigma} c^+_{i,-\sigma}|0\rangle \\
H_0 &= h_e + h_0 \\
h_1 &= \textstyle\sum_{i,j,\sigma} \Big((U_1 - J) c^+_{i,\sigma} c^+_{j,\sigma} c_{j,\sigma} c_{i,\sigma} \\
&\qquad + U_1 c^+_{i,\sigma} c^+_{j,-\sigma} c_{j,-\sigma} c_{i,\sigma} - J c^+_{i,\sigma} c^+_{j,-\sigma} c_{j,\sigma} c_{i,-\sigma} \Big) \\
U_1 &= \langle 0|c_{j,\sigma} c_{i,\sigma} V_{e-e} c^+_{i,\sigma} c^+_{j,\sigma}|0\rangle \\
J &= \langle 0|c_{j,\sigma} c_{i,-\sigma} V_{e-e} c^+_{i,\sigma} c^+_{j,-\sigma}|0\rangle \\
H_1 &= h_e + h_1
\end{aligned} \quad , \tag{2}$$

wherein U_0, U_1 and J designate[9] Coulomb and exchange integrals, respectively, and V_{e-e} refers to the electron-electron Coulomb potential.

The n-electron states make up a Hilbert space of dimension $d_0 = \begin{pmatrix} 2N \\ n \end{pmatrix}$, subtended by the basis $\{|I = 1, ..d_0\rangle\}$ with each $|I\rangle$ reading $|I\rangle = \prod_{j=1}^{n} c^+_{i_j,\sigma_j}|0\rangle$. The j^{th} electron, having spin σ_j, sits on the site i_j. The sites are ordered such that $i_j < i_{j+1}$, except in case of double occupancy, characterised by $i_j = i_{j+1}$ and $\sigma_j \sigma_{j+1} < 0$. Let us introduce now a sequence of n real numbers $k_{j=1,..n} \in [-\pi, \pi]$ and ϕ_1 defined as

$$\phi_1 = \sum_{I=1}^{d_0} e^{ik.I}|I\rangle \quad , \quad e^{ik.I} = e^{i\sum_{j=1}^{n} k_j r_{i_j}} \quad ,$$

with $r_{i=1,..N}$ being the position vector of site i.

The group of permutations P of n objects is assumed to act on ϕ_1 as follows

$$\phi_P = P\phi_1 = \sum_{I=1}^{d_0} e^{iPk.I}|I\rangle, e^{iPk.I} = e^{i\sum_{j=1}^{n} P(k_j) r_{i_j}},$$

wherein there is a one-to-one correspondence $k_j \xrightarrow{P} k_l = P(k_j)$ between $k_{j=1,..n}$ and $k_{l=1,..n}$. At last, the Hamiltonian H is projected onto the subspace, subtended by $n!$ of ϕ_P's, so that every eigenvector of H is found to read as a linear combination of the ϕ_P's

$$\psi = \sum_P x_P \phi_P = \sum_I \sum_P \left(x_P e^{iPk.I} \right) |I\rangle \quad , \tag{3}$$

wherein $n!$ of x_P's are complex numbers to be determined below. This last term on the right-hand side of Eq.(3) is recognised to be identical to the expression of Bethe's wave-function in Eq.(9) of [4]

 doi:10.20944/preprints202404.0124.v1

and extends thereby its validity to *any* $d = 1$ Hamiltonian, as illustrated below for H_1. However noteworthy is that $n!$ may become bigger than d_0 for n close to N, in which case the ϕ_P's are no longer linearly independent from one another.

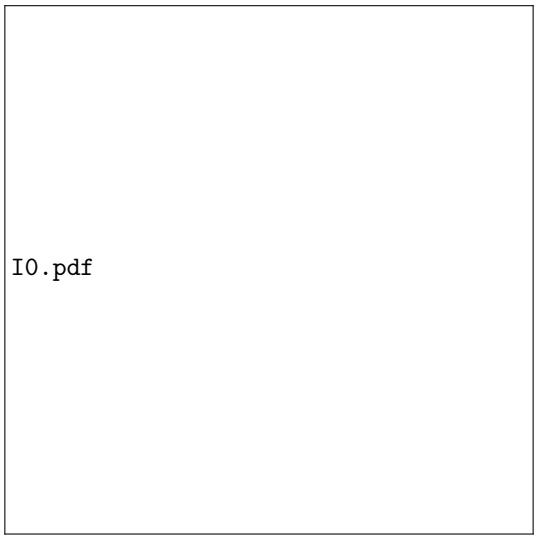

Figure 1. Sketch of $|I_0\rangle$, defined by Eqs.(4,8) for H_0, H_1, respectively, and sites $i = 1,..6$; dots and $+, -, \pm$ signs refer to an empty site or one accommodating either one electron of spin 1 or -1 or two electrons of opposite spin ± 1, respectively.

The expression of the eigenvalue ε_e, associated with ψ in Eq.(3), will now be worked out for $n \leq N$ in the case of the Hubbard Hamiltonian H_0. To that end, the particular n-electron state $|I_0\rangle$, sketched in Fig.1, is defined as

$$|I_0\rangle = \prod_{j=1}^{n} c^{+}_{j,(-1)^j}|0\rangle \quad , \tag{4}$$

while assuming the boundary conditions

$$\begin{array}{l} h_e|1,\sigma\rangle = -t(|2,\sigma\rangle + |N,\sigma\rangle) \\ h_e|N,\sigma\rangle = -t(|1,\sigma\rangle + |N-1,\sigma\rangle) \end{array} \quad . \tag{5}$$

Thus $|I_0\rangle$ is seen to have the properties

$$\begin{array}{l} \langle I_0|H_0|I_0\rangle = 0 \quad , \quad \left\langle I_0|H_0|I^{\pm}_j \right\rangle \neq 0 \Rightarrow \\ \left|I^{\pm}_{j=1,..n}\right\rangle = c^{+}_{j\pm 1,(-1)^j} c_{j,(-1)^j}|I_0\rangle \Rightarrow \\ \left\langle I_0|H_0|I^{\pm}_j \right\rangle = -t \quad , \quad e^{ik.I^{\pm}_j} = e^{\pm ik_j} e^{ik.I_0} \end{array} \quad . \tag{6}$$

Eq.(6) then entails

$$\begin{array}{c} \langle I_0|H_0|\phi_1\rangle = -te^{ik.I_0} \sum_{j=1}^{n} \left(e^{ik_j} + e^{-ik_j}\right) \\ = e^{ik.I_0} \sum_{j=1}^{n} \epsilon(k_j) \end{array} \quad ,$$

with $\epsilon(k_j)$ defined in Eq.(1). Extending this equation to every ϕ_P and applying it further to the Schrödinger equation $(H_0 - N\varepsilon_e)\psi = 0$, with ψ defined by Eq.(3), yields finally the energy per site ε_e as

$$\begin{array}{c} \langle I_0|H_0 - N\varepsilon_e|\psi\rangle = 0 \Rightarrow \\ \sum_{j=1}^{n} \frac{\epsilon(k_j)}{N} \sum_P x_P e^{iPk.I_0} = \varepsilon_e \sum_P x_P e^{iPk.I_0} \Rightarrow \\ \varepsilon_e = \sum_{j=1}^{n} \frac{\epsilon(k_j)}{N} \end{array} \quad . \tag{7}$$

 doi:10.20944/preprints202404.0124.v1

Proceeding for H_1 similarly as done for H_0, $|I_0\rangle$, sketched in Fig.1, will be defined for *even* $n \leq N$ as

$$|I_0\rangle = \prod_{j=1}^{n/2} c^+_{2j,+} c^+_{2j,-} |0\rangle \quad . \tag{8}$$

Assuming again the conditions in Eq.(5), $|I_0\rangle$ is inferred to have the properties

$$\begin{array}{l} \langle I_0|H_1|I_0\rangle = 0 \quad , \quad \left\langle I_0|H_1|I^{\pm}_{j,\pm}\right\rangle \neq 0 \\ \Rightarrow \left\{ \begin{array}{l} \left|I^{\pm}_{j=1,..\frac{n}{2},+}\right\rangle = c^+_{2j\pm1,+} c_{2j,+}|I_0\rangle \\ \left|I^{\pm}_{j=1,..\frac{n}{2},-}\right\rangle = c^+_{2j\pm1,-} c_{2j,-}|I_0\rangle \end{array} \right. \\ \Rightarrow \left\{ \begin{array}{l} \left\langle I_0|H_1|I^{\pm}_{j=1,..\frac{n}{2},\pm}\right\rangle = -t \\ e^{ik.I^{\pm}_{j=1,..\frac{n}{2},+}} = e^{\pm ik_{2j}} e^{ik.I_0} \\ e^{ik.I^{\pm}_{j=1,..\frac{n}{2},-}} = e^{\pm ik_{2j-1}} e^{ik.I_0} \end{array} \right. \end{array} \quad , \tag{9}$$

which entails for every P

$$\begin{array}{l} \langle I_0|H_1|\phi_P\rangle = -te^{iPk.I_0} \sum_{j=1}^{n} \left(e^{iP(k_j)} + e^{-iP(k_j)}\right) \\ \qquad\qquad = e^{iPk.I_0} \sum_{j=1}^{n} \epsilon(k_j) \end{array} \quad .$$

Taking advantage of $\langle I_0|H_1 - N\varepsilon_e|\psi\rangle = 0$, as done in Eq.(7), yields for ε_e the same expression as already given in Eq.(7). This latter expression of ε_e is recognised to be identical to Eq.(11) of [4]. Likewise, since it consists in a sum over one-particle energies, it is typical of a many-electron *scattering* state, so that the many *bound* electron states of H_0, H_1, addressed elsewhere[8], are left out of the purview of this work. Nevertheless it is worth noticing that ε_e could be achieved thanks to a careful, model dependent choice of $|I_0\rangle$ (see Eqs.(4,8)). Though ε_e is independent from the two-electron coupling, h_{e-e} will prove below quite instrumental in assigning the x_P values.

But before doing that, it is in order to derive the expression of the energy ε_h, valid for $n \in [N, 2N]$, by replacing electrons by holes. To that end, we begin with recasting h_e, h_0, h_1 as

$$\begin{array}{l} h_e = t \sum_{i,j,\sigma} \left(c_{j,\sigma} c^+_{i,\sigma} + c_{i,\sigma} c^+_{j,\sigma}\right) \\ h_0 = U_0 \sum_{i=1}^{N} c_{i,\sigma} c_{i,-\sigma} c^+_{i,-\sigma} c^+_{i,\sigma} \\ h_1 = \sum_{i,j,\sigma} \Big((U_1 - J) c_{i,\sigma} c_{j,\sigma} c^+_{j,\sigma} c^+_{i,\sigma} \\ \qquad + U_1 c_{i,\sigma} c_{j,-\sigma} c^+_{j,-\sigma} c^+_{i,\sigma} - J c_{i,-\sigma} c_{j,\sigma} c^+_{j,-\sigma} c^+_{i,\sigma} \Big) \end{array} \quad .$$

Any n-hole state $|I = 1,..d_0\rangle$ reads $|I\rangle = \prod_{j=1}^{n} c_{i_j,\sigma_j}|2\rangle$, with $|2\rangle$ characterised by each of N sites accommodating 2 electrons. Then substituting $|2\rangle$ to $|0\rangle$ in Eqs.(4,8) and $c_{j,\sigma}$ to $c^+_{j,\sigma}$ in Eqs.(4,6,8,9), and proceeding as done above for electrons yields the following expression for the energy per site of a n-hole state

$$\varepsilon_h = \varepsilon_h(2) - \sum_{j=1}^{n} \frac{\epsilon(k_j)}{N} \quad , \tag{10}$$

with $\varepsilon_h(2) = U_0$ and $\varepsilon_h(2) = 2(1 - \frac{1}{N})(2U_1 - J)$ being the energy per site of $|2\rangle$ for H_0 and H_1, respectively.

3. 2-Two-body scattering

The x_P coefficients will be assessed by analysing the two-body scattering, embodied by h_0, h_1. As a matter of fact, the latter turns out to be model dependent and to differ according to whether both electrons, partaking in the scattering process, have parallel or anti-parallel spin, which is referred to below as triplet or singlet case, respectively, for the sake of comparison with a previous work[7].

 doi:10.20944/preprints202404.0124.v1

The general procedure, used to calculate the x_P's, is to be sketched now. First a n-electron state $|J_0\rangle$ is culled in order to illustrate the two-body scattering. It can be seen in Fig.2 to differ from $|I_0\rangle$ in Fig.1, merely by both electrons, involved in the scattering process and located on sites $r_{j<4}$. Accordingly it is convenient to make use of transpositions T_{ij}, defined by $T_{ij}(k_i) = k_j, T_{ij}(k_j) = k_i, T_{ij}(k_{l\neq i,j}) = k_l$, which enables us to recast $A = \langle J_0|H - N\varepsilon_e|\psi\rangle = 0$, with ψ given by Eq.(3), as

$$\begin{array}{l} A = \sum_P B_P = 0 \\ B_P = \left\langle J_0|H - N\varepsilon_e|x_P\phi_P + x_{T_{12}P}\phi_{T_{12}P}\right\rangle \\ \quad\quad = x_P z_P + x_{T_{12}P} z_{T_{12}P} \\ z_Q = \sum_j e^{iQk.J_j}\langle J_0|H|J_j\rangle - N\varepsilon_e e^{iQk.J_0} \end{array} \quad , \tag{11}$$

wherein Q stands for $P, T_{12}P$ and the sum over P is to be carried out on $(n-2)!$ of pairs $\{P, T_{12}P\}$, whereas the subset of n-electron states $|J_j\rangle$ is characterised by $\langle J_0|H|J_j\rangle \neq 0$. Then $A = 0$ in Eq.(11) will be fulfilled by requiring

$$B_P = 0, \forall P \Rightarrow \frac{x_{T_{12}P}}{x_P} = -\frac{z_P}{z_{T_{12}P}} \quad . \tag{12}$$

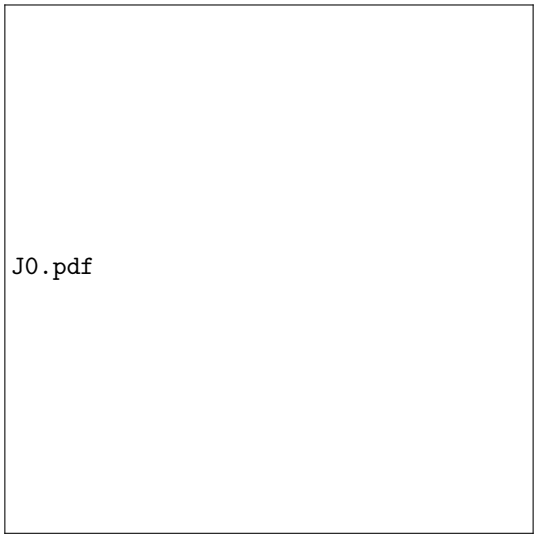

Figure 2. Sketch of $|J_0\rangle$ in Eqs.(13,16,18) and $|J_0^+\rangle$ in Eq.(20); the various symbols have the same meaning as in Fig.1.

- H_0**-triplet scattering** Taking $P(k_{j=1,..n<N-1}) = k_j$ for simplicity, because the final result will prove P independent, yields the following properties for the $|J_j\rangle$ states

$$\begin{array}{c} |J_0\rangle = c^+_{2,+}c^+_{3,+}\prod_{j=5}^{n+2} c^+_{j,(-1)^j}|0\rangle \\ \langle J_0|H_0|J_0\rangle = 0 \quad , \quad \left\langle J_0|H_0|J_j^{(\pm)}\right\rangle \neq 0 \Rightarrow \\ \left\{ \begin{array}{l} |J_1\rangle = c^+_{1,+}c_{2,+}|J_0\rangle \\ |J_4\rangle = c^+_{4,+}c_{3,+}|J_0\rangle \\ \left|J^\pm_{j>4}\right\rangle = c^+_{j\pm1,\sigma_j}c_{j,\sigma_j}|J_0\rangle \end{array} \right. \\ \langle J_0|H_0|J_{1,4}\rangle = \left\langle J_0|H_0|J^\pm_{j>4}\right\rangle = -t \\ e^{ik.J_1} = e^{-ik_1}e^{ik.J_0} \quad e^{ik.J_4} = e^{ik_2}e^{ik.J_0} \\ e^{ik.J^\pm_{j>4}} = e^{\pm ik_{j-2}}e^{ik.J_0} \end{array} \quad . \tag{13}$$

 doi:10.20944/preprints202404.0124.v1

In addition an important relationship between $e^{ik.J_0}, e^{iT_{12}k.J_0}$, valid also for H_1 triplet and singlet scattering, can be deduced from Eq.(13)

$$\frac{e^{ik.J_0}}{e^{iT_{12}k.J_0}} = \frac{e^{\frac{i}{2}(k_1r_2+k_2r_3)}}{e^{\frac{i}{2}(k_2r_2+k_1r_3)}} = \frac{e^{\frac{i}{2}(k_2-k_1)}}{e^{\frac{i}{2}(k_1-k_2)}} \quad . \tag{14}$$

Replacing $x_P, x_{T_{12}P}, z_P, z_{T_{12}P}$ by $x(k_1,k_2)$, $x(k_2,k_1)$, $z(k_1,k_2), z(k_2,k_1)$ and taking advantage of Eqs.(12,13,14) give

$$\begin{array}{c} \frac{z(k_1,k_2)}{z(k_2,k_1)} = \frac{e^{\frac{i}{2}(k_2-k_1)}}{e^{\frac{i}{2}(k_1-k_2)}} \frac{t\left(e^{-ik_1}+e^{ik_2}\right)+\epsilon(k_1)+\epsilon(k_2)}{t\left(e^{-ik_2}+e^{ik_1}\right)+\epsilon(k_1)+\epsilon(k_2)} \\ = \frac{e^{\frac{i}{2}(k_2-k_1)}}{e^{\frac{i}{2}(k_1-k_2)}} \frac{e^{ik_1}+e^{-ik_2}}{e^{ik_2}+e^{-ik_1}} = 1 \Rightarrow \frac{x(k_2,k_1)}{x(k_1,k_2)} = -1 \end{array} .$$

Applying this equation with any P, such that $P(k_1) = k_i, P(k_2) = k_j$, leads finally to $\frac{x\left(k_i,k_j\right)}{x\left(k_j,k_i\right)} = -1, \forall i,j \neq i$. Noteworthy is that $z(k_1,k_2), z(k_2,k_1)$ are found to be complex conjugate of each other, a property which will be seen to hold for all other kinds of two-body scattering investigated in this work. Therefore it is convenient to recast $\frac{x\left(k_i,k_j\right)}{x\left(k_j,k_i\right)} = -1$ as

$$\frac{x\left(k_i,k_j\right)}{x\left(k_j,k_i\right)} = e^{2i\theta_t\left(k_i,k_j\right)} \Rightarrow \theta_t\left(k_i,k_{j\neq i}\right) = \frac{\pi}{2}. \tag{15}$$

Remarkably, θ_t is constant and thence independent from t, U_0.

- H_0**-singlet scattering** Here are the properties of the $\left|J_j\right\rangle$ states

$$\begin{array}{c} |J_0\rangle = c^+_{2,+}c^+_{2,-}\prod_{j=4}^{n+1} c^+_{j,(-1)^j}|0\rangle \\ \left\langle J_0|H_0|J_j^{\pm}\right\rangle \neq 0 \Rightarrow \\ \left\{ \begin{array}{l} \left|J_1^{\pm}\right\rangle = c^+_{1,\pm}c_{2,\pm}|J_0\rangle \\ \left|J_3^{\pm}\right\rangle = c^+_{3,\pm}c_{2,\pm}|J_0\rangle \\ \left|J_{j>3}^{\pm}\right\rangle = c^+_{j\pm1,\sigma_j}c_{j,\sigma_j}|J_0\rangle \end{array} \right. \\ \langle J_0|H_0|J_0\rangle = U_0, \quad \left\langle J_0|H_0|J^{\pm}_{1,3,j>3}\right\rangle = -t \\ e^{ik.J_1^{\pm}} = e^{-ik_1}e^{ik.J_0}, \quad e^{ik.J_3^{\pm}} = e^{ik_2}e^{ik.J_0} \\ e^{ik.J_{j>3}^{\pm}} = e^{\pm ik_{j-1}}e^{ik.J_0} \end{array} . \tag{16}$$

It is inferred from $e^{ik.J_0} = e^{iT_{12}k.J_0}$ and Eq.(16)

$$\left.\begin{array}{l} \frac{z(k_1,k_2)}{z(k_2,k_1)} = \\ \frac{U_0-2t\left(e^{-ik_1}+e^{ik_2}\right)-\epsilon(k_1)-\epsilon(k_2)}{U_0-2t\left(e^{-ik_2}+e^{ik_1}\right)-\epsilon(k_1)-\epsilon(k_2)} = \\ \frac{U_0/t-e^{-ik_1}+e^{ik_1}-e^{ik_2}+e^{-ik_2}}{U_0/t-e^{ik_1}+e^{-ik_1}-e^{-ik_2}+e^{ik_2}} = \\ \frac{U_0/(2t)+i(\sin k_1-\sin k_2)}{U_0/(2t)-i(\sin k_1-\sin k_2)} \end{array}\right\} \Rightarrow$$
$$\frac{x(k_1,k_2)}{x(k_2,k_1)} = -\frac{z(k_2,k_1)}{z(k_1,k_2)} = \frac{\sin k_2-\sin k_1+iU_0/(2t)}{\sin k_2-\sin k_1-iU_0/(2t)}$$

Applying this equation with any P, as done in Eq.(15), leads finally to

$$\begin{array}{l} \frac{x\left(k_i,k_j\right)}{x\left(k_j,k_i\right)} = e^{2i\theta_s\left(k_i,k_j\right)} \Rightarrow \\ \tan\theta_s\left(k_i,k_{j\neq i}\right) = \frac{U_0}{2t\left(\sin k_j-\sin k_i\right)} \end{array} . \tag{17}$$

 doi:10.20944/preprints202404.0124.v1

Substituting the short-cut $x\left(k_i,k_j\right)$ to x_P is seen to be vindicated by $\theta_{t,s}\left(k_i,k_j\right)$ showing up indeed independent from every $k_{l\neq i,j}$ in Eqs.(15,17). This fortunate property could be established owing to a dedicated choice of $\left|J_0\right\rangle$.

- H_1**-triplet scattering** The properties of the $\left|J_j\right\rangle$ states are as follows for $n<N-1$

$$\begin{array}{l}
|J_0\rangle = c_{2,+}^{+}c_{3,+}^{+}\prod_{j=3}^{\frac{n}{2}+1}c_{2j,+}^{+}c_{2j,-}^{+}|0\rangle\\
\langle J_0|H_1|J_0\rangle = U_1-J\\
\left\langle J_0|H_1|J_{j>0,(\pm)}^{(\pm)}\right\rangle \neq 0 \Rightarrow\\
\left\{\begin{array}{l}
|J_1\rangle = c_{1,+}^{+}c_{2,+}|J_0\rangle\\
|J_4\rangle = c_{4,+}^{+}c_{3,+}|J_0\rangle\\
\left|J_{j>2,+}^{\pm}\right\rangle = c_{2j\pm1,+}^{+}c_{2j,+}|J_0\rangle\\
\left|J_{j>2,-}^{\pm}\right\rangle = c_{2j\pm1,-}^{+}c_{2j,-}|J_0\rangle
\end{array}\right.\\
\langle J_0|H_1|J_{1,4}\rangle = \left\langle J_0|H_1|J_{j>2,\pm}^{\pm}\right\rangle = -t\\
e^{ik.J_1} = e^{-ik_1}e^{ik.J_0},\quad e^{ik.J_4} = e^{ik_2}e^{ik.J_0}\\
e^{ik.J_{j>2,+}^{\pm}} = e^{\pm ik_{2j-2}}e^{ik.J_0}\\
e^{ik.J_{j>2,-}^{\pm}} = e^{\pm ik_{2j-3}}e^{ik.J_0}
\end{array}. \tag{18}$$

Since Eq.(14) applies to this case too, it is inferred from Eq.(18)

$$\begin{array}{l}
\frac{z(k_1,k_2)}{z(k_2,k_1)} = \frac{e^{\frac{i}{2}(k_2-k_1)}}{e^{\frac{i}{2}(k_1-k_2)}}\frac{t\left(e^{-ik_1}+e^{ik_2}\right)-U_1+J+\epsilon(k_1)+\epsilon(k_2)}{t\left(e^{-ik_2}+e^{ik_1}\right)-U_1+J+\epsilon(k_1)+\epsilon(k_2)}\\
= \frac{e^{\frac{i}{2}(k_2-k_1)}-\frac{2t}{U_1-J}\cos\left(\frac{k_1+k_2}{2}\right)}{e^{\frac{i}{2}(k_1-k_2)}-\frac{2t}{U_1-J}\cos\left(\frac{k_1+k_2}{2}\right)} \Rightarrow \frac{x\left(k_j,k_i\right)}{x\left(k_i,k_j\right)}\\
= \frac{\sin\left(\frac{k_i-k_j}{2}\right)+i\left(\cos\left(\frac{k_i-k_j}{2}\right)-\frac{2t}{U_1-J}\cos\left(\frac{k_i+k_j}{2}\right)\right)}{\sin\left(\frac{k_i-k_j}{2}\right)-i\left(\cos\left(\frac{k_i-k_j}{2}\right)-\frac{2t}{U_1-J}\cos\left(\frac{k_i+k_j}{2}\right)\right)}\\
= e^{2i\theta_t\left(k_i,k_j\right)}
\end{array}, \tag{}$$

which yields finally for $\theta_t\left(k_i,k_j\right)$

$$\tan\theta_t\left(k_i,k_{j\neq i}\right) = \frac{\cos\frac{k_i-k_j}{2}-\frac{2t}{U_1-J}\cos\left(\frac{k_i+k_j}{2}\right)}{\sin\left(\frac{k_i-k_j}{2}\right)}. \tag{19}$$

 doi:10.20944/preprints202404.0124.v1

- H_1**-singlet scattering** The properties of the $|J_j\rangle$ states are as follows

$$
\begin{gathered}
|J_0^+\rangle = c_{2,+}^+ c_{3,-}^+ \prod_{j=3}^{\frac{n}{2}+1} c_{2j,+}^+ c_{2j,-}^+ |0\rangle \\
|J_0^-\rangle = c_{2,-}^+ c_{3,+}^+ \prod_{j=3}^{\frac{n}{2}+1} c_{2j,+}^+ c_{2j,-}^+ |0\rangle \\
\langle J_0^+|H_1|J_0^+\rangle = U_1 \quad \langle J_0^+|H_1|J_0^-\rangle = -J \\
\left\langle J_0^+|H_1|J_{j>0,(\pm)}^{(\pm)}\right\rangle \neq 0 \Rightarrow \\
\left\{ \begin{array}{l}
|J_1\rangle = c_{1,+}^+ c_{2,+}|J_0^+\rangle \\
|J_2\rangle = c_{2,-}^+ c_{3,-}|J_0^+\rangle \\
|J_3\rangle = c_{3,+}^+ c_{2,+}|J_0^+\rangle \\
|J_4\rangle = c_{4,-}^+ c_{3,-}|J_0^+\rangle \\
\left|J_{j>2,+}^{\pm}\right\rangle = c_{2j\pm1,+}^+ c_{2j,+}|J_0^+\rangle \\
\left|J_{j>2,-}^{\pm}\right\rangle = c_{2j\pm1,-}^+ c_{2j,-}|J_0^+\rangle
\end{array} \right. \\
\langle J_0^+|H_1|J_{1,..4}\rangle = \left\langle J_0^+|H_1|J_{j>2,\pm}^{\pm}\right\rangle = -t \\
e^{ik.J_0^-} = e^{ik.J_0^+} \\
e^{ik.J_1} = e^{-ik_1} e^{ik.J_0^+}, e^{ik.J_3} = e^{ik_1} e^{ik.J_0^+} \\
e^{ik.J_2} = e^{-ik_2} e^{ik.J_0^+}, e^{ik.J_4} = e^{ik_2} e^{ik.J_0^+} \\
e^{ik.J_{j>2,+}^{\pm}} = e^{\pm ik_{2j-2}} e^{ik.J_0} \\
e^{ik.J_{j>2,-}^{\pm}} = e^{\pm ik_{2j-3}} e^{ik.J_0}
\end{gathered}
\tag{20}
$$

Since Eq.(14) is valid in this case too, it is inferred from Eq.(20)

$$
\begin{gathered}
\frac{z(k_1,k_2)}{z(k_2,k_1)} = \frac{e^{\frac{i}{2}(k_2-k_1)}}{e^{\frac{i}{2}(k_1-k_2)}} \times \\
\frac{U_1-J-t\left(e^{ik_1}+e^{-ik_1}+e^{ik_2}+e^{-ik_2}\right)-\epsilon(k_1)-\epsilon(k_2)}{U_1-J-t\left(e^{ik_1}+e^{-ik_1}+e^{ik_2}+e^{-ik_2}\right)-\epsilon(k_1)-\epsilon(k_2)} \\
= \frac{e^{\frac{i}{2}(k_2-k_1)}}{e^{\frac{i}{2}(k_1-k_2)}} \Rightarrow \frac{x(k_j,k_i)}{x(k_i,k_j)} = -\frac{e^{\frac{i}{2}(k_j-k_i)}}{e^{\frac{i}{2}(k_i-k_j)}} = e^{2i\theta_s(k_i,k_j)}
\end{gathered}
,
$$

which yields finally for $\theta_s(k_i,k_j)$

$$
\theta_s(k_i,k_{j\neq i}) = \frac{\pi - k_i + k_j}{2} \quad . \tag{21}
$$

Unlike θ_t in Eq.(19), θ_s shows up independent from t, U_1, J.

4. 3-Boundary condition

The hereabove results will be taken advantage of, in order to show that the $k_{i=1,..n}$'s are related to one another through a boundary condition, ensueing from Eq.(5). To that end, the permutations P_1, P_N and n-electron states $|I_1\rangle, |I_N\rangle$ are needed

$$
\begin{gathered}
\left.\begin{array}{l}
P_1(k_{i=1,..n}) = k_i \\
P_N(k_{i=1,..n-1}) = k_{i+1}, \quad P_N(k_n) = k_1
\end{array}\right\} \Rightarrow \\
P_N = \prod_{j=2}^{n} T_{1j} P_1 \Rightarrow x_{P_N} = e^{2i\sum_{j=2}^{n}\theta_\beta(k_1,k_j)} x_{P_1} \\
\left.\begin{array}{l}
|I_1\rangle = \prod_{j=1}^{n} c_{j,\sigma_j}^+ |0\rangle \\
|I_N\rangle = c_{N,\sigma_1}^+ c_{1,\sigma_1}|I_1\rangle
\end{array}\right\} \Rightarrow \frac{e^{iP_N k.I_N}}{e^{iP_1 k.I_1}} = e^{iNk_1}
\end{gathered}
\quad , \tag{22}
$$

 doi:10.20944/preprints202404.0124.v1

with $\sigma_{j=1,..n-1}\sigma_{j+1} > 0\ (< 0)$ for $\beta = t\ (\beta = s)$. Besides, it is convenient to take the sequence $\{k_{i=1,..n}\}$, such that $k_{i=1,..n-1} < k_{i+1}$. Then the sought boundary condition reads by substituting $T_{1i}P_1, T_{i1}P_N$ to P_1, P_N in Eq.(22) and applying it further to any $k_{i>1}$

$$\begin{array}{l} x_{P_1}e^{iP_1k.I_1} = x_{P_N}e^{iP_Nk.I_N} \Rightarrow \\ e^{i\left(Nk_{i=1,..n}+2\sum_{j=1}^{n}\theta_\beta(k_i,k_{j\neq i})\right)} = 1 \Rightarrow \\ k_i = 2\pi\alpha_{i=1,..n} - \frac{2}{N}\sum_{j=1}^{n}\theta_\beta(k_i,k_{j\neq i}) \end{array} \quad , \tag{23}$$

with $\alpha_{i=1,..n} = \frac{m_i}{N}$ and the integers $m_{i=1,..n} \in [1,N] \Rightarrow \alpha_{i=1,..n} \in [0,1]$. At last taking the limit $N \to \infty, n \to \infty, \frac{n}{N} \to c_0 \in [0,1]$ yields

$$\begin{array}{l} k(\alpha \in [0,1]) = 2\pi\alpha - 2\int_{-\pi}^{\pi}\theta_\beta(k,u)\rho_\beta(u)du \\ \rho_\beta(k)dk = d\alpha \Rightarrow \\ \rho_\beta(k) = \frac{d\alpha}{dk} = \frac{1}{2\pi} + \int_{-\pi}^{\pi}\frac{\partial\theta_\beta}{\partial k}(k,u)\rho_\beta(u)\frac{du}{\pi} \\ \varepsilon_\beta = \int_{-\pi}^{\pi}\epsilon(k)\rho_\beta(k)dk \quad , \quad c_0 = \int_{-\pi}^{\pi}\rho_\beta(k)dk \end{array} \quad , \tag{24}$$

for which $c_0, \varepsilon_{\beta=t,s}, \rho_\beta(k)$ stand for the whole electron concentration, *triplet* or *singlet* energy per site and corresponding one-electron density of states, respectively. Though each eigenvalue $\varepsilon_{\beta=t,s}$ is seen to read as a sum over one-particle energies $\epsilon(k)$, as is the case for independent electrons[9], there is a one to one correspondence between ε_β and its associated, h_{e-e}-dependent $\rho_\beta(k)$, whereas the density of states is *unique* for all many independent electron states. Moreover, since each eigenvector ψ is defined by a *unique* sequence $\{k_{i=1,..n}\}$, two different eigenvectors do not even belong in the same vector space, because their respective $\{k_{i=1,..n}\}$-dependent bases $\{\phi_P\}$ are thence linearly independent from each other.

Solving Eq.(24) for the groundstate energy will be done below as follows

$$\begin{array}{l} \rho_\beta(k) = \frac{1}{2\pi} + \int_{-k_\beta}^{k_\beta}\frac{\partial\theta_\beta}{\partial k}(k,u)\rho_\beta(u)\frac{du}{\pi} = \frac{1}{2\pi} + \\ \int_0^{k_\beta}\left(\frac{\partial\theta_\beta}{\partial k}(k,u)\rho_\beta(u) + \frac{\partial\theta_\beta}{\partial k}(k,-u)\rho_\beta(-u)\right)\frac{du}{\pi} \end{array} \quad , \tag{25}$$

with $k_\beta \in [0,\pi]$. Besides Eqs.(15,17,19,21) imply

$$\frac{\partial\theta_\beta}{\partial k}(k,u) = \frac{\partial\theta_\beta}{\partial k}(-k,-u), \frac{\partial\theta_\beta}{\partial k}(k,-u) = \frac{\partial\theta_\beta}{\partial k}(-k,u),$$

whence it is inferred $\rho_\beta(k) = \rho_\beta(-k)$, so that Eq.(25) can be recast as

$$\rho_\beta(k) = \frac{1}{2\pi} + \int_0^{k_\beta} g_\beta(k,u)\rho_\beta(u)\frac{du}{\pi} \quad , \tag{26}$$

with $g_\beta(k,u) = \frac{\partial\theta_\beta}{\partial k}(k,u) + \frac{\partial\theta_\beta}{\partial k}(k,-u)$. By discretising $[0,k_\beta] \Rightarrow k_{j=1,..m} = \frac{j-1}{m-1}k_\beta$ and calculating the integral in Eq.(26) with help of Simpson's rule, Eq.(26) will be eventually solved below for $\rho_\beta(k)$, as a Cramer system, comprising m equations in terms of the unknowns $\rho_\beta(k_{j=1,..m})$, while $\frac{\partial\theta_t}{\partial k}(k,u)$, $\frac{\partial\theta_s}{\partial k}(k,u)$ are taken from Eq.(15),Eq.(17) (Eq.(19),Eq.(21)), respectively, in case of H_0 (H_1). Finally the groundstate energy ε_g is achieved by reckoning $c_t, \varepsilon_t, c_s, \varepsilon_s$ as follows

$$\begin{array}{l} c_\beta(k_{\beta=t,s}) = 2\int_0^{k_\beta}\rho_\beta(k)dk \\ \varepsilon_\beta(k_\beta) = 2\int_0^{k_\beta}\epsilon(k)\rho_\beta(k)dk \end{array} \quad . \tag{27}$$

Assigning the values of $k_t(c_0), k_s(c_0)$ thanks to the constraint $c_t = c_s = c_0$ gives finally access to $\varepsilon_g(c_0)$ as the lower of $\varepsilon_t(k_t(c_0)), \varepsilon_s(k_s(c_0))$.

 doi:10.20944/preprints202404.0124.v1

5. 4-Groundstate energy for H_0

θ_t being constant in Eq.(15) entails via Eq.(26) $\rho_t(k) = \frac{1}{2\pi}, \forall k$, which further implies thanks to Eq.(27)

$$\left.\begin{array}{l} c_t = \frac{k_t}{\pi} \\ \varepsilon_t = -\frac{2t}{\pi}\sin k_t \end{array}\right\} \Rightarrow \varepsilon_t(c_t) = -\frac{2t}{\pi}\sin(\pi c_t), \tag{28}$$

which shows up independent from U_0. The $\varepsilon_t(c_0), \varepsilon_s(c_0)$ data have been plotted in Fig.3. The inequality $\varepsilon_s(c_0 \in [0,1]) < \varepsilon_t(c_0)$ can be seen to hold for any $\frac{U_0}{t}$ value. A comparison with groundstate energies $\eta_1(c_0)$, reckoned with a previous version of Bethe's wave-function[6], reveals that the inequality $\varepsilon_s(c_0) < \eta_1(c_0)$ is found to hold for $\frac{U_0}{t} < 4$, whereas the opposite one $\varepsilon_s(c_0) > \eta_1(c_0)$ is observed for $\frac{U_0}{t} > 4$. Actually this discrepancy results from $\varepsilon_s(c_0)$ being calculated for *singlet* electrons only, whereas $\eta_1(c_0)$ has been worked out for a mixture of *singlet* and *triplet* electrons. Therefore it can be explained as follows: the smaller $\frac{U_0}{t}$ is, the bigger $\rho_s(k)$ is with respect to $\rho_t(k) = \frac{1}{2\pi}$ for $k < \frac{\pi}{2}$, so that refraining from mixing *singlet* and *triplet* electrons causes $\varepsilon_s(c_0) < \eta_1(c_0)$. Contrarily, $\varepsilon_s(c_0)$ is seen to merge into $\varepsilon_t(c_0)$ for $\frac{U_0}{t} \to \infty$, because of $\theta_s(k_i, k_j) \to \theta_t = \frac{\pi}{2}$ as seen in Eqs.(15,17). Consequently, $\frac{U_0}{t} \to \infty$ entails that $\rho_s(k < \frac{\pi}{2}) \to \rho_t, \rho_s(k > \frac{\pi}{2}) < \rho_t$, so that the *singlet-triplet* mixture favours eventually the opposite conclusion $\eta_1(c_0) < \varepsilon_s(c_0)$ for $\frac{U_0}{t} > 4$.

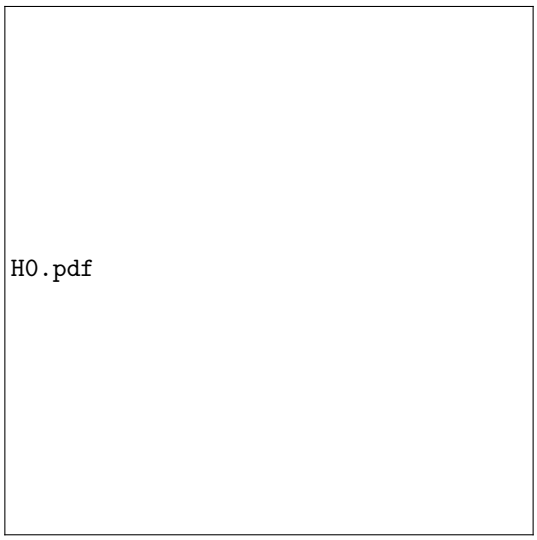

Figure 3. Plots of $\varepsilon_t(c_0)$, as given in Eq.(28) (white square), $\varepsilon_s(c_0)$ (solid line, dashed line, dotted line, dashed-dotted line) and $\eta_1(c_0)$ (white triangle, white circle, white diamond, $\times$), calculated for H_0 with $\gamma = \frac{U_0}{t} = 1, 2, 4, 8$, as said in the text.

Furthermore it is in order to compare ε_s with the electronic energy η_2, obtained with help of the correlated Fermi gas (*CFG*) model[7] in normal metals, the characteristic features of which will be recalled now for self-containedness. Each *independent*-electron band of dispersion $\epsilon(k \in [-\pi, \pi])$, as given in Eq.(1), accommodating at most 2 electrons of opposite spin direction per site, splits into one *singlet* and one *triplet* band, each of them accommodating at most 1 electron per site. The corresponding dispersion curves $\epsilon_s(k), \epsilon_t(k)$ read for the general Hamiltonian H as follows

$$\left.\begin{array}{l} \epsilon_t(k) = \sum_{k'} \left\langle 0 \middle| c_{k,\sigma} c_{k',\sigma} H c^+_{k',\sigma} c^+_{k,\sigma} \middle| 0 \right\rangle \\ \epsilon_s(k) = \sum_{k'} \left\langle 0 \middle| c_{k,\sigma} c_{k',-\sigma} H c^+_{k',-\sigma} c^+_{k,\sigma} \middle| 0 \right\rangle \end{array}\right. , \tag{29}$$

for which $\left\langle 0 \middle| c_{k,\sigma} c^+_{k,\sigma} \middle| 0 \right\rangle = \left\langle 0 \middle| c_{k',\pm\sigma} c^+_{k',\pm\sigma} \middle| 0 \right\rangle = 1$ has been assumed and $c^+_{k,\sigma}, c_{k,\sigma}$ are one-electron creation and annihilation operators on the Bloch[9] state $|k,\sigma\rangle$

$$|k,\sigma\rangle = c^+_{k,\sigma}|0\rangle \quad , \quad |0\rangle = c_{k,\sigma}|k,\sigma\rangle \quad .$$

 doi:10.20944/preprints202404.0124.v1

Besides, the calculation requires the expression of H in momentum space, which will be taken from a previous work[8] for illustration in case of H_0, H_1. Note that $\epsilon_t(k), \epsilon_s(k)$ are found in general to depend not only on h_{e-e} but also on the concentration of singlet or triplet electrons c_s, c_t and there is $\epsilon_t(k) = \epsilon_t(-k), \epsilon_s(k) = \epsilon_s(-k)$. Then both *singlet* and *triplet* bands are populated in accordance with Fermi-Dirac statistics[9], which yields in the $d = 1$ case at $T = 0K$

$$\begin{array}{l} c_s = \frac{k_s}{\pi}, \quad \eta_s = \int_0^{k_s} \epsilon_s(k) \frac{dk}{\pi}, \quad \epsilon_s(k_s) = E_F \\ c_t = \frac{k_t}{\pi}, \quad \eta_t = \int_0^{k_t} \epsilon_t(k) \frac{dk}{\pi}, \quad \epsilon_t(k_t) = E_F \\ c_0 = c_s + c_t \quad , \quad \eta_2(c_0) = \eta_s(c_s) + \eta_t(c_t) \end{array} \quad , \tag{30}$$

with E_F, η_s, η_t standing for the Fermi energy[9] and the partial *singlet* and *triplet* energy, respectively.

The expressions of $\epsilon_t, \eta_t, \epsilon_s, \eta_s$ are recalled[7] to read for the Hubbard model

$$\begin{array}{l} \epsilon_t(k) = \epsilon(k), \quad \eta_t = -\frac{2t}{\pi} \sin k_t \\ \epsilon_s(k) = \epsilon(k) + U_0 \frac{c_s}{2}, \quad \eta_s = -\frac{2t}{\pi} \sin k_s + U_0 \frac{c_s^2}{2} \end{array} .$$

Unlike $\varepsilon_s \neq \eta_1$, the energies η_1, η_2 have been found[7] quite close to each other, namely there is $\left| 1 - \frac{\eta_1(c_0, \frac{U_0}{t})}{\eta_2(c_0, \frac{U_0}{t})} \right| < .01$ for all $c_0, \frac{U_0}{t}$-values. As a matter of fact this agreement is all the more baffling, since η_1 is a true eigenvalue, whereas η_2 comes out of a variational calculation, and furthermore the associated eigen- and variational many-electron states belong in quite different vector spaces. Hence this unexpected feature is likely to stem from both states comprising *singlet* and *triplet* electrons.

6. 5-Groundstate energy for H_1

$\frac{\partial \theta_s}{\partial k}(k, u) = -.5$ is inferred from Eq.(21) to be constant, which entails owing to Eq.(26) that $\rho_s(k) = \frac{1}{2(k_s + \pi)}$ is constant too, and eventually thanks to Eq.(27)

$$\begin{array}{l} c_s = \frac{k_s}{k_s + \pi} \Rightarrow \\ \varepsilon_s = -\frac{2t}{k_s + \pi} \sin k_s = -\frac{2t}{\pi} (1 - c_s) \sin\left(\frac{\pi c_s}{1 - c_s} \right) \end{array} . \tag{31}$$

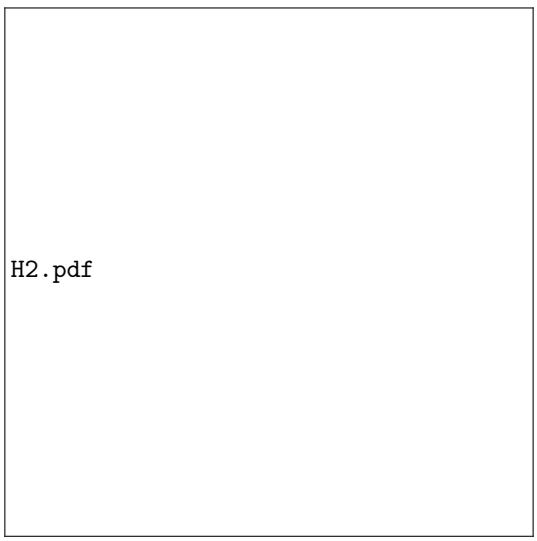

Figure 4. Plots of $\varepsilon_s(c_0)$, as given in Eq.(31) (white square), $\varepsilon_t(c_0)$ (solid line, dashed line, dotted line, dashed-dotted line) and $\eta_2(c_0)$ (white triangle, white circle, white diamond, $\times$), calculated for H_1 with $\gamma = \frac{U_1 - J}{t} = 1, .75, .5, .25$ and $J = .1U_1$, as said in the text.

 doi:10.20944/preprints202404.0124.v1

It results from Eq.(31) that $c_s \leq .5$ and $\varepsilon_s(c_s)$ shows up independent from $U_1 - J$. As a matter of fact, there is no meaningful ε_t solution either, i.e. with $\rho_t(k) > 0, \forall k$, for $c_t > .5$. The $\varepsilon_t, \varepsilon_s$ data, plotted in Fig.4, show that the inequality $\varepsilon_t(c_0) < \varepsilon_s(c_0)$ holds for all γ-values.

Implementing Eqs.(29,30) for H_1 yields

$$\begin{array}{l} \epsilon_t(k) = \epsilon(k) + (U_1 - J)\left(c_t + \frac{\sin(k-k_t)-\sin(k+k_t)}{2\pi}\right) \\ \eta_t = -\frac{2t}{\pi}\sin k_t + (U_1 - J)\left(c_t^2 + \frac{\cos(2k_t)-1}{2\pi^2}\right) \\ \epsilon_s(k) = \epsilon(k) + U_1 c_s + J\frac{\sin(k+k_s)-\sin(k-k_s)}{\pi} \\ \eta_s = -\frac{2t}{\pi}\sin k_s + U_1 c_s^2 + J\frac{1-\cos(2k_s)}{\pi^2} \end{array} .$$

The η_2 data have been plotted in Fig.4. The inequality $\eta_2(c_0) < \varepsilon_t(c_0)$ is seen to hold for all $c_0 < .5$ values and is likely to ensue again from the *CFG* state, including *triplet* and *singlet* electrons with $c_t \approx c_s \approx \frac{c_0}{2}, \forall c_0$, by contrast with Bethe's wave-function of eigenvalue $\varepsilon_t(c_0)$ comprising only *triplet* electrons.

7. 6-Discussion

Since the groundstate is widely believed to describe the properties of any physical system at $T = 0K$, it is of significance to sort, out of the various many electron states, discussed hereabove, that one, likely to account at best for the observed properties of interacting electrons. To that end, it should be noticed that all of them share a common property, namely the total energy ε consists in a sum over one-*fermion* energy either $\epsilon(k)$ or $\epsilon_{\beta=s,t}(k)$. Thus, the groundstate can be built[9] by populating every one-electron state from the bottom of the one-electron band, corresponding to $\epsilon(k = 0)$, up to a c_0 dependent upper bound, designated as the Fermi energy E_F. The reader can check that this requirement is met by all kinds of many-electron states of concern hereabove, i.e. Bethe's wave-function and *CFG* states. However Fermi-Dirac statistics requires in addition at $T = 0K$ that the relationship $E_F = \frac{\partial \varepsilon}{\partial c_0}$ hold[9,10]. Obviously solely the *CFG* solution meets successfully this constraint, because it obeys Fermi-Dirac statistics by definition (see $E_F = \epsilon_t(k_t) = \epsilon_s(k_s)$ in Eq.(30)), whereas there is $E_F \neq \frac{\partial \varepsilon}{\partial c_0}$ for all kinds of Bethe's wave-functions, studied here and elsewhere[3,4,6]. Yet, as seen above, the *CFG* solution is *not* the groundstate for H_0 in case of $\frac{U_0}{t} < 4$.

Buttressing the claim that the *CFG* state is observable would help validate this analysis. To that end, let us discuss electron spin resonance (*ESR*) in case of H_1. Applying an external magnetic field H lifts[11] the degeneracy between the respective energies of one-electron states $\epsilon_\pm(k)$ of $c^+_{k,+}\left|0\right\rangle$, $c^+_{k,-}\left|0\right\rangle$ for *triplet* electrons as follows

$$\begin{array}{l} \epsilon_\pm(k) = f(k, k_\pm(H)) \pm \frac{\mu H}{2} \\ f(k_\pm(H), k_\pm(H)) \pm \frac{\mu H}{2} = E_F(H) \end{array} ,$$

for which μ stands for the electron magnetic moment and there is $f(x, y) = \epsilon_t(x)$, taken from Eq.(29) with $x = k$ and $y = k_\pm(H)$ instead of k_t in case of $H \neq 0$, which thence implies $f(k_t, k_t) = E_F(H = 0)$. Then the experiment consists of measuring the absorption of a resonant electromagnetic field of frequency ω, such that $\hbar\omega = f(k_+, k_+) - f(k_+, k_-)$, which implies

$$\omega = \left(1 + \frac{\frac{\partial f}{\partial y}(k_t, k_t)}{\frac{\partial f}{\partial x}(k_t, k_t) + \frac{\partial f}{\partial y}(k_t, k_t)}\right)\frac{\mu H}{\hbar} \quad . \tag{32}$$

Remarkably the *singlet* electrons are seen not to contribute to the *ESR* signal, because their associated many-electron state is *not* degenerate at $H = 0$, due to the electrons of spin $\pm\sigma$ keeping *same* concentration $= \frac{c_s}{2}$ even for $H \neq 0$. Actually the *ESR* signal has been observed[11] but in a paucity of cases, namely alcali, noble metals and *Al* at $\frac{\omega}{H} \approx 3\text{GHz/KG}$. This might stem from $\frac{\partial f}{\partial x}(k_t, k_t) + \frac{\partial f}{\partial y}(k_t, k_t) \approx 0$

 doi:10.20944/preprints202404.0124.v1

in Eq.(32), which would shift ω upward at fixed H. Hopefully this work might kindle attempts at seeking the *ESR* signal in the *IF* rather than microwave range, as done usually[11] with $H < 10KG$.

8. Conclusion

Bethe's wave-function has been shown to subtend the subspace of scattering eigenstates of the $d = 1$ Hubbard Hamiltonian. Though this analysis is independent of a previous one[3,4], both pieces of work lead to the same conclusions, summarised by Eqs.(3,7). The two-body scattering plays a key role. Likewise, though the Coulomb force does not depend on the spin of both electrons, involved in the scattering process, its outcome *does* indeed (see Eqs.(15,17,19,21)), as a consequence of Pauli's principle. This analysis can be applied to any realistic $d = 1$ Hamiltonian, which has been exemplified on H_1. Nevertheless Bethe's wave-function turns out to be of limited significance in condensed matter physics, because it has been shown not to be *observable*. Actually, the groundstate can be observed at $T = 0K$ solely for atoms, molecules and insulators. Conversely it cannot in superconducting and magnetic compounds and in normal metals, because, as argued elsewhere[7], there are two kinds of conduction electrons at thermal equilibrium with one another in each case, namely normal versus superconducting, normal versus magnetic and *triplet* versus *singlet* electrons, respectively.

Acknowledgments: One of us (J.S.) is beholden to Michel Abou Ghantous for help and encouragement.

References

1. Bethe H. Z.Phys. 71 1931 205
2. Mattis D.C. The Theory of Magnetism I Springer Verlag, New-York 1981
3. Gaudin M. La Fonction d'Onde de Bethe Masson, Paris 1983
4. Lieb E.H.Wu F.Y. Physica A 321 2003 1 (also available in *arXiv* : condmat/0207529)
5. Szeftel J., Moudden H. Kocharian A. J.Magn.Magn.Mat. 187 1998 261
6. Shiba H. Phys.Rev.B 6 1972 930
7. Szeftel J. J.Supercond.Nov.Magn. 35 2022 689
8. Szeftel J. J.Supercond.Nov.Magn. 35 2022 3085
9. Ashcroft N.W. Mermin N. D. Solid State Physics Saunders College 1976
10. Landau L.D. Lifshitz E.M. Statistical Physics Pergamon Press, London 1959
11. Weil J.A.Bolton J.R. Electron Paramagnetic Resonance: Elementary Theory and Practical Applications John Wiley & Sons 2007